Influence of Alkoxy Tail Length on the Self-Organization of Hairy-Rod Polymers Based on Mesogen-Jacketed Liquid Crystalline Polymers

Sheng Chen, Changkai Jie, Helou Xie, Hailiang Zhang

Key Laboratory of Polymeric Materials and Application Technology of Hunan Province, and Universities of Hunan Province, College of Chemistry, Xiangtan University, Xiangtan 411105, Hunan Province, China
Correspondence to: H. Zhang (E-mail: hailiangzhang1965@yahoo.com.cn)

Received 10 May 2012; accepted 21 May 2012; published online 00 Month 2012
DOI: 10.1002/pola.26194

ABSTRACT: A series of hairy-rod polymers, poly{2,5-bis[(4-alkoxyphenyl)oxycarbonyl]styrenes} (P-OC*m*, $m = 1, 2, 4, 6, 8, 10, 12, 14, 16$, and 18) were designed and successfully synthesized via free radical polymerization. The chemical structure of the monomers was confirmed by elemental analysis, ^{1}H NMR and ^{13}C NMR. The molecular characterizations of the polymers were performed with ^{1}H NMR and gel permeation chromatography. The phase structures and transitions of the polymers were investigated by the combination of techniques including differential scanning calorimetry, wide-angle X-ray diffraction, polarized optical microscopy, and rheological measurement. The experimental results revealed that the self-assembly behaviors of P-OC*m* changed with the increase in *m*. First, the P-OC*m* ($m = 1, 2$) showed only a stable liquid crystalline phase above T_g. Second, with the increasing length of alkoxy tails, the P-OC*m* ($m = 4, 6, 8$) presented a re-entrant isotropic phase above T_g and a liquid crystalline phase at higher temperature. Third, the P-OC*m* ($m = 10, 12, 14, 16, 18$) exhibited an unusual re-entrant isotropic phase which was separating SmA (in low temperature) and columnar phases (in high temperature). It was the first time that mesogen-jacketed liquid crystalline polymers formed smectic phase, re-entrant isotropic phase, and columnar phases in one polymer due to the microphase separation and the driving force of the entropy. © 2012 Wiley Periodicals, Inc. J Polym Sci Part A: Polym Chem 000: 000–000, 2012

KEYWORDS: hairy-rod polymers; mesogen-jacketed liquid crystalline polymer (LCP); phase behavior; re-entrant isotropic phase; rheology; self-organization

INTRODUCTION Self-assembly, nanophase separation, and confinement are widely researched in multicomponent soft systems because soft matter is very important for functional materials science and biosystems.[1–4] So the design, synthesis, and self-assembly behaviors of soft materials is a hot topic of research,[5–9] especially liquid crystalline polymers. In liquid crystalline polymers' systems, as well known, the rigidity of polymers is formed not only by the rigid backbone but also by some polymers with flexible backbone, such as mesogen-jacketed liquid crystalline polymers (MJLCPs) and dendronized polymers.[10–22] The MJLCP was first proposed by Zhou et al.[23,24] in the late 1980s to describe a novel type of side-chain liquid crystal polymer (side-chain LCPs) whose bulky mesogenic groups were laterally attached to the flexible backbone via a single or several carbon–carbon bonds. As a result, the strong steric hindrance imposed by the highly crowded bulky and rigid side groups around backbone forces the main-chain to be well extended, leading to the rod-like chain, which has been confirmed by small-angle neutron scattering technique. All those make MJLCPs exhibit special properties similar to those of rigid backbone polymers, such as high glass transition temperature, broad temperature range of mesophase, long persistence length in good solvent, and forming banded texture after mechanical shearing in LC state. As the concept of MJLCPs was proposed, rod-like MJLCP chains have tended to self-organize into different columnar LC phases with the polymer chains aligned parallel to one another, such as columnar nematic (Φ_H),[25,26] hexatic columnar nematic (Φ_{HN}),[26–29] two-dimensional (2D) hexagonal columnar phases (2D Φ_H)[30] and rectangular columnar (Φ_R) phase.[31] The type of these columnar phases depends on the molecular properties including the shape, size, and flexibility of side chains. Recently, smectic phases with the backbones embedded in the smectic layers have also been reported when the length or the rigidity of the mesogen was increased or when semifluorinated tails or hydrogen bonding were introduced into the mesogens.[32,33] As can be seen, the MJLCPs normally shows the smectic phase or columnar phase, however, it hard forms smectic phase and columnar phase in one polymer with the

Additional Supporting Information may be found in the online version of this article.

temperature improved because it is difficult to simultaneously meet the requirements of the forming of two kinds of liquid crystal phase.

In the rigid-rod polymers' systems, most of polymers contain the rigid backbone, such as aromatic polyesters,[34–36] polyamides,[37–39] polyanilines,[40,41] and poly(3-alkylthiophene).[42,43] However, there are some disadvantages (such as high melting points, low solubility, low compatible with thermoplastic polymers) for the rigid backbone polymers which hinder the further research. To overcome such defects, one way is the attachment of flexible alkyl side chains to the polymer rigid backbone. One thinks that the rigid polymer can dissolve in the background of the side chains due to the (infinite) attractive interaction between the solvent molecules and the backbone, without loss of the rigidity of the backbone.[44–47] Moreover, due to microphase separation of the aliphatic and aromatic domains,[48–51] the rigid-rod polymers with different flexible alkyl side chains (hairy-rod polymers)[52] has led to not only the finding of the interesting structural feature in liquid crystalline phases but also the well organization of the polymers into highly oriented crystals. For example, the α-helical poly(γ-alkyl L-glutamates), aromatic polyesters, and polyamides with long alkyl side chains as the type of hairy-rod polymers can form multiple kinds of LC phaes,[48,51,53–55] such as hexagonal and lamellar microphase. Subsequently, some theoretical treatments have been presented and they pointed that hexagonal, oblique, and lamellar microphase separated structures as well as isotropic phase can form because of the balance between unfavorable rod–coil interaction and elastic stretching of the side chains based on the assumption about absence of rotational disordering.[52] In side-chain liquid crystalline polymer systems, the mesomorphic properties of side-chain LCPs are determined by the type of backbone, spacer, mesogenic group, the length of alkyl tail, molecular weight, and its distribution, and so forth. Especially, when the flexible spacers and alkyl tail length increase, side-chain LCPs are inclined to form smectic phase due to microphase separation.[56] From the properties of two types of polymers, the microphase separation leads to the formation of layer structure. So, a simple question arises as to what kind of properties are newly induced if long alkyl groups are attached to MJLCPs and whether MJLCPs can form smectic phase and columnar phase in one polymer.

As for the phase behavior of MJLCPs with different length alkyl tail, it has been reported before. For example, Chen et al.[57,58] reported a kind of MJLCPs with unbalanced mesogenic core and different terminal flexible substituents. When the carbon number for the flexible substituents were shorter than four (butoxy groups), well-defined S_A phase kept unchanged; whereas the one reached four, well-defined S_C phase was observed. Recently, Zhang et al.[59] also has researched the properties of MJLCPs containing biphenyl mesogen with asymmetric substitutions, poly(alkyl 4′-(octyloxy)-2-vinylbiphenyl-4-carboxylate) (pVBP(m,8)). When $m = 1$, the polymer was not liquid crystalline. All other polymers showed columnar liquid crystalline phase. Moreover, when the MJLCPs had balanced mesogenic core and different terminal flexible substituents, it exhibited more interesting LC phases structures, like poly{2,5-bis[(4-methoxyphenyl)oxycarbonyl]styrene} with terminal methoxy could form columnar nematic (Φ_N) and Φ_{HN} when the molecular weights increased,[26] but the polymers with long length of alkoxy tails exhibited another the interesting phase behavior which was quite similar to re-entrant isotropic phase, such as poly{2,5-bis[(4-butoxyphenyl)oxycarbonyl]styrene}, poly{2,5-bis[(4-hexyloxyphenyl)oxycarbonyl]styrene}, and poly{2,5-bis[(4-octoxyphenyl)oxycarbonyl]styrene} with a butoxy, hexyloxy, and octoxy, respectively.[60] The author pointed that the LC phase in high temperature was proposed to form by the driving force of the entropy, and the whole molecular motion was involved in the formation of the LC phase. Although the experimental results showed that the length of alkoxy tails had played an important role in the phase behaviors of MJLCPs, the MJLCPs did not exhibit smectic phase and columnar phase in one polymer. However, it can be seen that some MJLCPs can display a thermodynamically stable isotropic phase at lower temperature and a columnar phase at higher temperature. In addition, based on above literature survey, hairy-rod polymers and side-chain LCPs with long alkyl tail can present lamellar structure due to microphase separation. So, combined the microphase separation nature of hairy-rod polymers and side-chain LCPs with long alkyl tail with the driving force of the entropy nature of MJLCPs, it may simultaneously meet the requirements of the forming of two kinds of liquid crystal phase in the MJLCPs' systems.

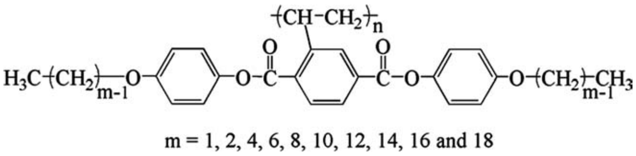

SCHEME 1 Chemical structures of the polymers (P-OC*m*).

Therefore, to systemically study the influence of the different length of terminal flexible substituents on phase behaviors of MJLCPs with balanced mesogenic core, we designed and synthesized a series of side-chain rigid-rod polymers with different length of alkoxy tails: poly{2,5-bis[(4-alkoxyphenyl)oxycarbonyl]styrenes} (P-OC*m*, *m* is the number of the carbons in the alkoxy groups, $m = 1$, 2, 4, 6, 8, 10, 12, 14, 16, and 18). The chemical structures of the polymers are shown in Scheme 1. More specifically, through the investigation of P-OC*m*, we can obtain some knowledge about the thermal behavior and the arrangement mode of molecular chain of P-OC*m* and can get the information of the structure variation of MJLCPs and pocking mode molecular chain.

In this work, we described the synthesis of the monomers and the corresponding homopolymers as well as the phase behaviors of the polymers. From our experimental results, these polymers can be divided into three types. The first type is that polymers show the transitional MJLCP phase behavior when they have short alkoxy terminals containing

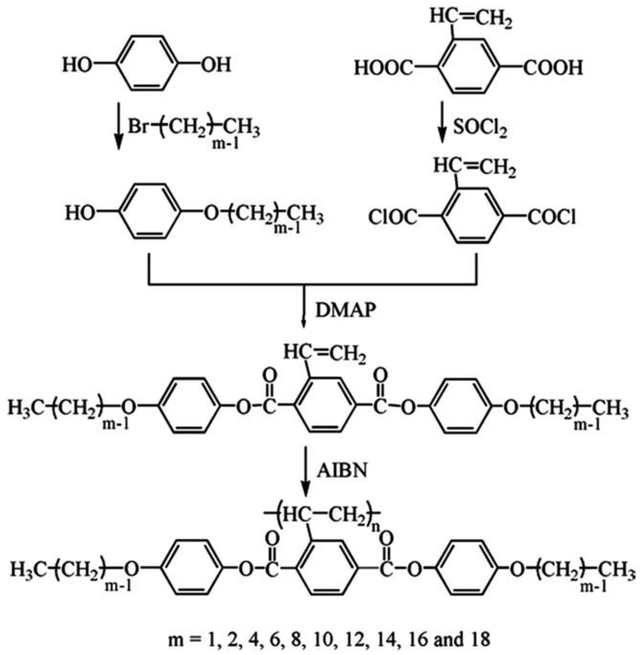

SCHEME 2 Synthetic route of the monomers (M-OC*m*) and the corresponding polymers (P-OC*m*).

one and two carbon atoms. The second type is that the P-OC*m* ($m = 4$, 6, and 8) presents a re-entrant isotropic phase and a LC phase. In MJLCPs, it is difficult to observe clearing transition because most of the MJLCPs decomposes before reaching its transition temperature from liquid crystal phase to isotropic phase ("clearing point"), so the occurrence of a re-entrant isotropic phase of MJLCPs has based on the assumption that it can observe one isotropic phase in high temperature. They are considered to be the first kind of MJLCPs with a re-entrant phase. The third type is that the P-OC*m* ($m = 10$, 12, 14, 16, and 18) exhibits a re-entrant isotropic phase which is separating SmA and columnar phases. They are considered to be the second kind of MJLCPs with a re-entrant phase. To our best of our knowledge, the MJLCPs can form the smectic phase and the columnar phase with the increase in temperature, which is first reported in the MJLCPs system. Compared to the re-entrant isotropic behavior of MJLCPs in the past, this article reported that the re-entrant isotropic phase was separating the smectic phase and the columnar phases. Moreover, due to the competing between the smectic phase and the columnar phases over a specific temperature range, the appearance and disappearance of the re-entrant isotropic phase are influenced by it. In all, the length of alkoxy tails greatly affect the packing behaviors of MJLCPs.

EXPERIMENTAL

Materials

The precursor 2-vinylterephthalic acid (VTA) was synthesized according to previous paper.[61,62] The *p*-(*n*-alkoxyl)phenols were prepared as described by Klarmann et al.[63] Chlorobenzene (Acros, 99%) was purified by washing with concentrated sulfuric acid to remove residual thiophenes, followed by washing twice with distilled water, once with 5% sodium carbonate solution, and again with distilled water before being dried with anhydrous calcium chloride and then distilled. 4-(Dimethylamino)pyridine (DMAP, 99%, ACROS), hydroquinone (98%, Alfa Aesar) and the corresponding alkyl bromides together with other reagents and solvents were used as received without further purification.

Synthesis of Monomers and Polymers

The synthesis of P-OC*m* ($m = 1$, 2, 4, 6, and 8) has been reported by our group and the synthetic route of monomers and the corresponding polymers are shown in Scheme 2 ($m = 1$, 2, 4, 6, 8, 10, 12, 14, 16, and 18). The experimental details are described as follows using 2,5-bis[(4-decyloxyphenyl)oxycarbonyl]styrene (M-OC_{10}) as an example: VTA (5.2 mmol, 1 g) was added into 30 mL of dried thionyl chloride in a 100-mL three-necked flask, then the mixture was refluxed. After VTA was dissolved absolutely, the excess thionyl chloride was removed under reduced pressure. The residue was washed with petroleum ether for three times. The petroleum ether was removed under the reduced pressure and afforded yellow liquid. This liquid was dissolved in dried THF to obtain solution A. P-decyloxyphenol (13.0 mmol, 3.26 g) and DMAP (26.0 mmol, 3.18 g) were dissolved in 20 ml of dried THF to obtain solution B. Under intense stirring at 0 °C, the solution A was slowly added into the solution B over a period of 2 h. The mixture was further stirred at room temperature for 12 h, and then, most of the THF was distilled off the system by evaporation under reduced pressure. After water was added into the residue, the crude solid product was first collected by filtration and dried under vacuum, and then purified using column chromatography on silica gel with chloroform as eluent. The product was further purified by recrystallization from chloroform/methanol (yield 71%). The characterization data of these monomers were as follows: ^{1}H NMR ($CDCl_3$): $\delta = 0.88–1.84$ (m, 38H, alkoxy H), 3.96–4.00 (t, 4H, $—O\mathit{CH_2}—$), 5.48–5.87 (2d, 2H, $=\mathit{CH_2}$), 6.95–7.17 (m, 8H, *Ar-H*), 7.53–7.60 (q, 1H, $—\mathit{CH}—$), 8.17–8.45 (m, 3H, *Ar-H*). ^{13}C NMR ($CDCl_3$): $\delta = 14.11$ ($—\mathit{CH_3}$), 22.69 ($—\mathit{CH_2}—$), 26.07 ($—\mathit{CH_2}—$), 29.31–29.60 ($—\mathit{CH_2}—$), 31.92 ($—\mathit{CH_2}—$), 68.51 ($—O\mathit{CH_2}—$), 115.21 ($=\mathit{CH_2}$), 118.35–122.26 (aromatic *C* ortho to *C*—O), 128.63 (aromatic *C*), 129.03 (aromatic *C*), 130.91 (aromatic *C*), 132.04 (aromatic *C*), 133.23 (aromatic *C*), 134.72 ($—\mathit{HC}=\mathit{CH_2}$), 140.49 (aromatic $\mathit{C}—HC=CH_2$), 144.00–144.10 (aromatic *C*—O), 157.14 (aromatic *C*—O), 164.59–165.39 (*C*=O). ($C_{42}H_{56}O_6$) (656.41): Calcd. C 76.79, H 8.59; Found C 76.50, H 8.60.

All the other monomers were synthesized and characterized similarly. The characterization data of M-OCm ($m = 12$, 14, 16, and 18) were as follows:

2,5-Bis[(4-dodecyloxyphenyl)oxycarbonyl]styrene (M-OC_{12})

^{1}H NMR ($CDCl_3$): $\delta = 0.89–1.84$ (m, 46H, alkoxy H), 3.98–4.00 (t, 4H, $—O\mathit{CH_2}—$), 5.48–5.88 (2d, 2H, $=\mathit{CH_2}$), 6.95–7.17 (m, 8H, *Ar-H*), 7.53–7.60 (q, 1H, $—\mathit{CH}=$), 8.17–8.45 (m, 3H, *Ar-H*). ^{13}C NMR ($CDCl_3$): $\delta = 14.11$ ($—\mathit{CH_3}$), 22.70 ($—\mathit{CH_2}—$), 26.07 ($—\mathit{CH_2}—$), 29.31–29.68 ($—\mathit{CH_2}—$), 31.94 ($—\mathit{CH_2}—$), 68.53 ($-OCH_2-$), 115.23 ($=CH_2$), 118.36–122.26 (aromatic *C* ortho to *C*—O), 128.64 (aromatic *C*), 129.05 (aromatic *C*), 130.92 (aromatic *C*), 132.06 (aromatic *C*), 133.24 (aromatic *C*), 134.72 ($-HC=CH_2$), 140.50 (aromatic *C*—HC$=$CH$_2$), 144.01–144.11 (aromatic *C*—O), 157.16 (aromatic *C*—O), 164.62–165.42 (*C*$=$O). ($C_{46}H_{64}O_6$) (712.47): Calcd. C 77.49, H 9.05; Found C 76.60, H 9.13.

2,5-Bis[(4-tetradecyloxyphenyl)oxycarbonyl]styrene (M-OC$_{14}$)

^{1}H NMR ($CDCl_3$): $\delta = 0.91$–1.81 (m, 54H, alkoxy H), 3.96–4.00 (t, 4H, $-OCH_2-$), 5.48–5.88 (2d, 2H, $=CH_2$), 6.95–7.17 (m, 8H, *Ar-H*), 7.53–7.60 (q, 1H, $-CH=$), 8.19–8.45 (m, 3H, *Ar-H*). ^{13}C NMR ($CDCl_3$): $\delta = 14.11$ ($-CH_3$), 22.70 ($-CH_2-$), 26.07 ($-CH_2-$), 29.31–29.68 ($-CH_2-$), 31.95 ($-CH_2-$), 68.53 ($-OCH_2-$), 115.23 ($=CH_2$), 118.36–122.26 (aromatic *C* ortho to *C*—O), 128.64 (aromatic *C*), 129.05 (aromatic *C*), 130.92 (aromatic *C*), 132.06 (aromatic *C*), 133.24 (aromatic *C*), 134.72 ($-HC=CH_2$), 140.50 (aromatic *C*—HC$=$CH$_2$), 144.01–144.11 (aromatic *C*—O), 157.16 (aromatic *C*—O), 164.62–165.41 (*C*$=$O). ($C_{50}H_{72}O_6$) (768.53): Calcd. C 78.08, H 9.44; Found C 77.83, H 9.62.

2,5-Bis[(4-hexadecyloxyphenyl)oxycarbonyl]styrene (M-OC$_{16}$)

^{1}H NMR ($CDCl_3$): $\delta = 0.87$–1.84 (m, 62H, alkoxy H), 3.97–4.00 (t, 4H, $-OCH_2-$), 5.48–5.87 (2d, 2H, $=CH_2$), 6.95–7.17 (m, 8H, *Ar-H*), 7.53–7.60 (q, 1H, $-CH=$), 8.19–8.45 (m, 3H, *Ar-H*). ^{13}C NMR ($CDCl_3$): $\delta = 14.11$ ($-CH_3$), 22.70 ($-CH_2-$), 26.07 ($-CH_2-$), 29.30–29.71 ($-CH_2-$), 31.95 ($-CH_2-$), 68.74 ($-OCH_2-$), 115.23 ($=CH_2$), 118.36–122.26 (aromatic *C* ortho to *C*—O), 128.65 (aromatic *C*), 129.05 (aromatic *C*), 130.92 (aromatic *C*), 132.06 (aromatic *C*),133.24 (aromatic *C*), 134.73 ($-HC=CH_2$), 140.50 (aromatic *C*—HC$=$CH$_2$), 144.01–144.11 (aromatic *C*—O), 157.16 (aromatic *C*—O), 164.62–165.42 (*C*—O). ($C_{54}H_{80}O_6$) (824.60): Calcd. C 78.60, H 9.77; Found C 78.31, H 10.19.

2,5-Bis[(4-octadecanalkoxylphenyl)oxycarbonyl]styrene (M-OC$_{18}$)

^{1}H NMR ($CDCl_3$): $\delta = 0.86$–1.86 (m, 70H, alkoxy H), 3.97–4.00 (t, 4H, $-OCH_2-$), 5.48–5.87 (2d, 2H, $=CH_2$), 6.95–7.17 (m, 8H, *Ar-H*), 7.53–7.60 (q, 1H, $-CH=$), 8.18–8.44 (m, 3H, *Ar-H*). ^{13}C NMR ($CDCl_3$): $\delta = 14.11$ ($-CH_3$), 22.70 ($-CH_2-$), 26.08 ($-CH_2-$), 29.31–29.712 ($-CH_2-$), 31.95 ($-CH_2-$), 68.75 ($-OCH_2-$), 115.23 ($=CH_2$), 118.36–122.26 (aromatic *C* ortho to *C*—O), 128.65 (aromatic *C*), 129.05 (aromatic *C*), 130.92 (aromatic *C*), 132.07 (aromatic *C*), 133.25 (aromatic *C*), 134.73 ($-HC=CH_2$), 140.51 (aromatic *C*—HC$=$CH$_2$), 144.02–144.12 (aromatic *C*—O), 157.17 (aromatic *C*—O), 164.62–165.42 (*C*$=$O). ($C_{58}H_{88}O_6$) (880.66): Calcd. C 79.04, H 10.06; Found C 79.08, H 10.55.

All the polymers were synthesized by conventional solution radical polymerization. For example, 0.656 g (1 mmol) of M-OC10, 100 μL of chlorobenzene solution of 0.01 mmol AIBN, 2 mL of chlorobenzene, and a magnetic stir bar were added into a polymerization tube, the tube was purged with nitrogen and subjected to four freeze–thaw cycles to remove any dissolved oxygen and sealed off under vacuum. Polymerization was carried out at 70 °C for 24 h. The tube was then opened, and the reaction mixture was diluted with 10 mL of THF. The resultant polymer was precipitated and washed with methanol. To eliminate the unreacted monomers completely, the purification was repeated, until no peak was observed at the elution time of monomer in gel permeation chromatography (GPC) measurement.

Instruments and Measurements

Elemental analysis was performed on an Elementar Vario EL instrument. All NMR measurements were performed on a Bruker ARX400 MHz spectrometer using $CDCl_3$ as solvent, tetramethylsilane as the internal standard at room temperature.

The apparent number-average molecular weight (M_n) and polydispersity index (PDI $= M_w/M_n$) were measured on a GPC (WATERS 1515) instrument with a set of HT3, HT4, and HT5. The μ-styragel columns used THF as an eluent and the flow rate was 1.0 mL/min at 38 °C. All the GPC data were calibrated with polystyrene standards.

TGA was performed on a TA-SDT 2960 instrument at a heating rate of 20 °C/min in nitrogen atmosphere.

DSC traces of all the polymers were obtained using a TA-Q10 DSC instrument. The temperature and heat flow were calibrated using standard materials (indium and zinc) at a cooling and heating rates of 10 °C/min. Samples with a typical mass of about 5 mg were encapsulated in sealed aluminum pans.

LC texture of the polymers was examined under polarized optical microscopy (POM) (Leica DM-LM-P) equipped with a Mettler-Toledo hot stage (FP82HT).

One-dimensional (1D) wide-angle X-ray diffraction (WAXD) experiments were performed on a Philips X'Pert Pro diffractometer with a 3-kW ceramic tube as the X-ray source (Cu Kα) and an X'celerator detector. The sample stage was set horizontally. The reflection peak positions were calibrated with silicon powder ($2\theta > 15°$) and silver behenate ($2\theta < 10°$). A temperature control unit (Paar Physica TCU 100) in conjunction with the diffractometer was used to study the structure evolutions as a function of temperature. To keep the equilibrium of systems, we kept a testing temperature for 40 min when heating or cooling the samples.

A Rheometrics ARES rheometer (TA ARES rheometer) was applied to measure the viscoelastic properties of the samples based on oscillatory shear. The experimental temperature was controlled using forced N_2 gas convection. Isochronal temperature scans were performed using a 20-mm diameter parallel-plate geometry with a frequency of 10 rad/s and a small strain amplitude. Isothermal frequency sweeps were made using the same setup at frequencies from 0.1 to 100 rad/s.

RESULTS AND DISCUSSION

Synthesis and Characterization of Monomers and Polymers

All the monomers could be easily polymerized via free radical polymerization method. Herein, we use P-OC10 as an

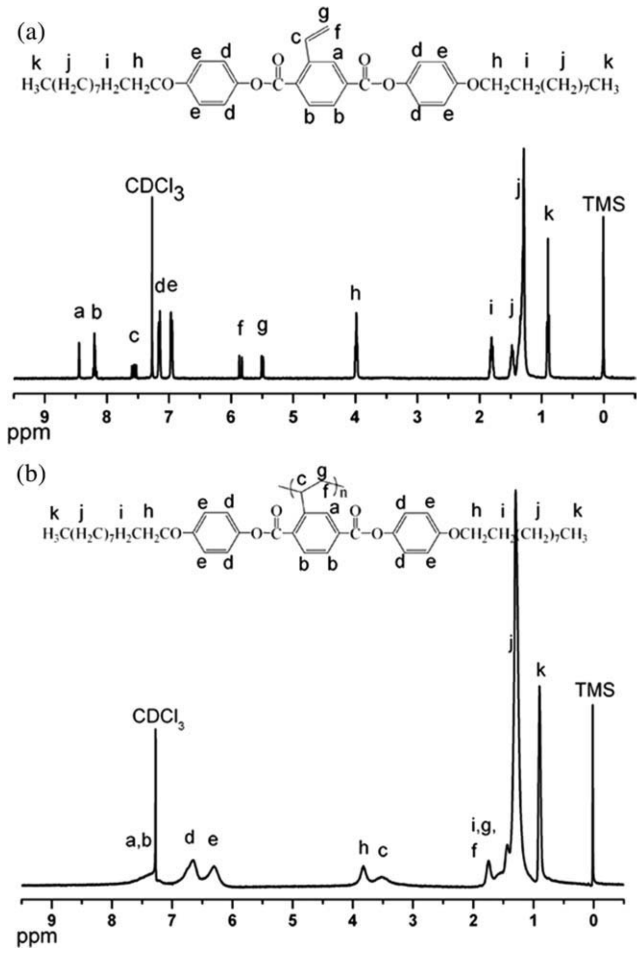

FIGURE 1 ^{1}H NMR spectrums of the monomer M-OC10 (a) and the polymer P-OC10 (b) in $\mathrm{CDCl_3}$.

example to elucidate the process. Figure 1(a,b) give the ^{1}H NMR spectra (CDCl_3^{-d}) of the monomer M-OC10 and the polymer P-OC10, respectively. The M-OC10 showed the characteristic resonances of the vinyl group at 5.48–5.87 and 7.53–7.60 ppm. After polymerization, these signals disappeared completely. The chemical shifts of P-OC10 were quite broad and consistent with the expected polymer structure. To remove the influence of M_n on the LC behaviors, we synthesized a series of polymers with the similar M_n. All the polymers showed good thermal stability, that is, the temperatures at 5% weight loss of the samples under nitrogen were about 400 °C measured by TGA at a rate of 10 °C/min. The molecular characterizations of the polymers are summarized Table 1.

Phase Transitions and Phase Structures of the Polymers

The phase behaviors of the monomers M-OC*m* were examined by the conventional analyses including DSC and POM. All the monomers can form LC phase during the heating and cooling processes, but the monomers would suffer thermal polymerization, so the mesophase was not stable. Therefore, we mainly discuss the phase behaviors of polymers hereinafter. DSC experiments revealed that the melting point of M-OC*m* ($m = 1$, 2, 4, 6, 8, 10, 12, 14, 16, and 18) were measured to be 111.1, 121.5, 107.7, 66.0, 79.2, 79.4, 87.5, 94.9, 95.5, and 100.3 °C, respectively.

Figure 2 shows the first cooling and the second heating DSC curves of P-OC*m* ($m = 1$, 2, 4, 6, 8, 10, 12, 14, 16, and 18) at a rate of 10 °C/min under nitrogen atmosphere after eliminating the thermal history. On the basis of transitional phenomenon of the polymers, the curves in Figure 2(a) can be divided into three types. The first one, there is no transition peak except a glass transition (T_g) to be observed in the curves in the P-OC*m* ($m = 1$ and 2). The second one, all the samples exhibit a single transition peak in high temperature region above T_g when *m* becomes 4, 6, or 8. These two types are well agreement with the previous papers.[60,62] However, the last one, the samples with more longer length of alkoxy tails ($m = 10$, 12, 14, 16, and 18) exhibit more special transitional peaks, that is, besides the transitional peak in high temperature, there are two transition peaks that appeared in the lower temperature region and in slightly above the corresponding T_g. These two transition peaks correspond to the crystallization of the long alkoxy tails and to the interconversion between isotropic phase and new LC phase, respectively. The corresponding transitions were observed during the second heating process [see Fig. 2(b)], indicating the reversible transitions for the polymers.

From the experiment results, we can observe that the alkoxy tails of the P-OC*m* can be crystallized when the number of carbon atoms in the side groups exceeds 10. Melting points

TABLE 1 Molecular Characteristics of Polymers

Sample	$M_n(\times10^{-5})$[a]	PDI[a]	T_g [b](°C)	$T_d(N_2)$(°C)[c]	T_1(°C)[d]	T_2(°C)[e]
P-OC1	3.13	2.21	120	396	–	–
P-OC2	2.03	1.78	112	398	–	–
P-OC4	2.31	1.98	102	406	–	169
P-OC6	2.28	2.05	100	391	–	203
P-OC8	3.10	2.31	105	418	–	200
P-OC10	2.12	2.22	109	416	130	252
P-OC12	2.50	1.96	108	418	130	253
P-OC14	2.80	2.12	104	424	131	247
P-OC16	2.03	2.21	101	409	123	258
P-OC18	3.92	1.88	92	408	113	218
P-OC18[f]	2.22	2.21	91	409	118	242

[a] Relative M_n and PDI were measured by GPC using PS standards.

[b] The glass transition temperatures were measured by DSC at a heating rate of 10 °C/min under nitrogen atmosphere during the second heating process.

[c] The temperatures at 5% weight loss of the samples under nitrogen [$T_d(N_2)$] were measured by TGA heating experiments at a rate of 10 °C/min.

[d] The transition temperature from first liquid crystalline phase to isotropic phase measured by DSC at a heating rate of 10 °C/min under nitrogen atmosphere during the second heating process.

[e] The transition temperature from isotropic phase to the second liquid crystalline phase measured by DSC at a heating rate of 10 °C/min under nitrogen atmosphere during the second heating process.

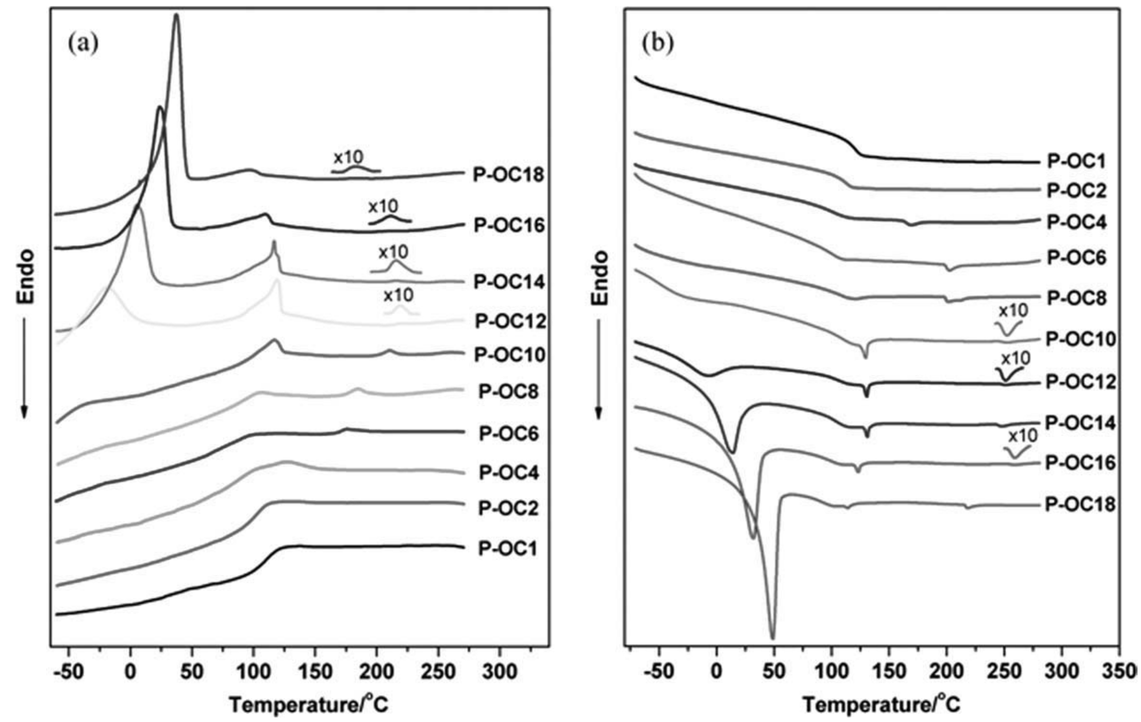

FIGURE 2 DSC curves of P-OC*m* during the first cooling scan (a) and the second heating scan (b) at a rate of 10 °C/min under nitrogen atmosphere.

of the alkoxy tails of P-OC*m* increase with the increasing length of alkyl, moreover, a comparison of the melting points (T_m) of the alkoxy tails with those of *n*-alkanes [see Fig. 3(a)] shows that the T_m of alkoxy tails are significantly higher than the melting points of the same length *n*-alkanes. As well known to all, the side chains of the comb-like polymers have been found to be crystallized in hexagonal form, such as poly(*n*-alkyl itaconate)s, *N*-alkylated poly(p-benzamide),[64] poly(octadecyl acrylate),[65] and so on. So, we thought the long alkoxy tails of the P-OC*m* can also be crystallized in hexagonal form. After melting of the paraffin crystallites, the alkyl side chains were from ordered packing to disordered packing.

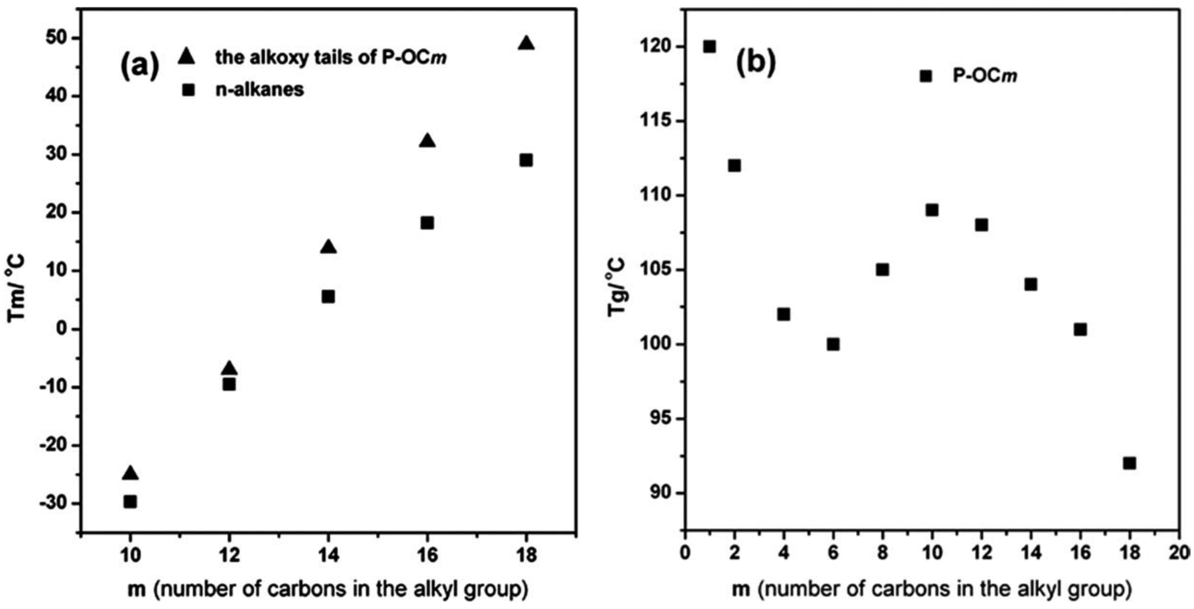

FIGURE 3 (a) The influence of alkyl length on the melting points of the alkoxy tails of P-OC*m* and *n*-alkanes (C_mH_{2m+2}) and (b) the influence of alkyl length on the glass transition temperature (T_g) of P-OC*m*.

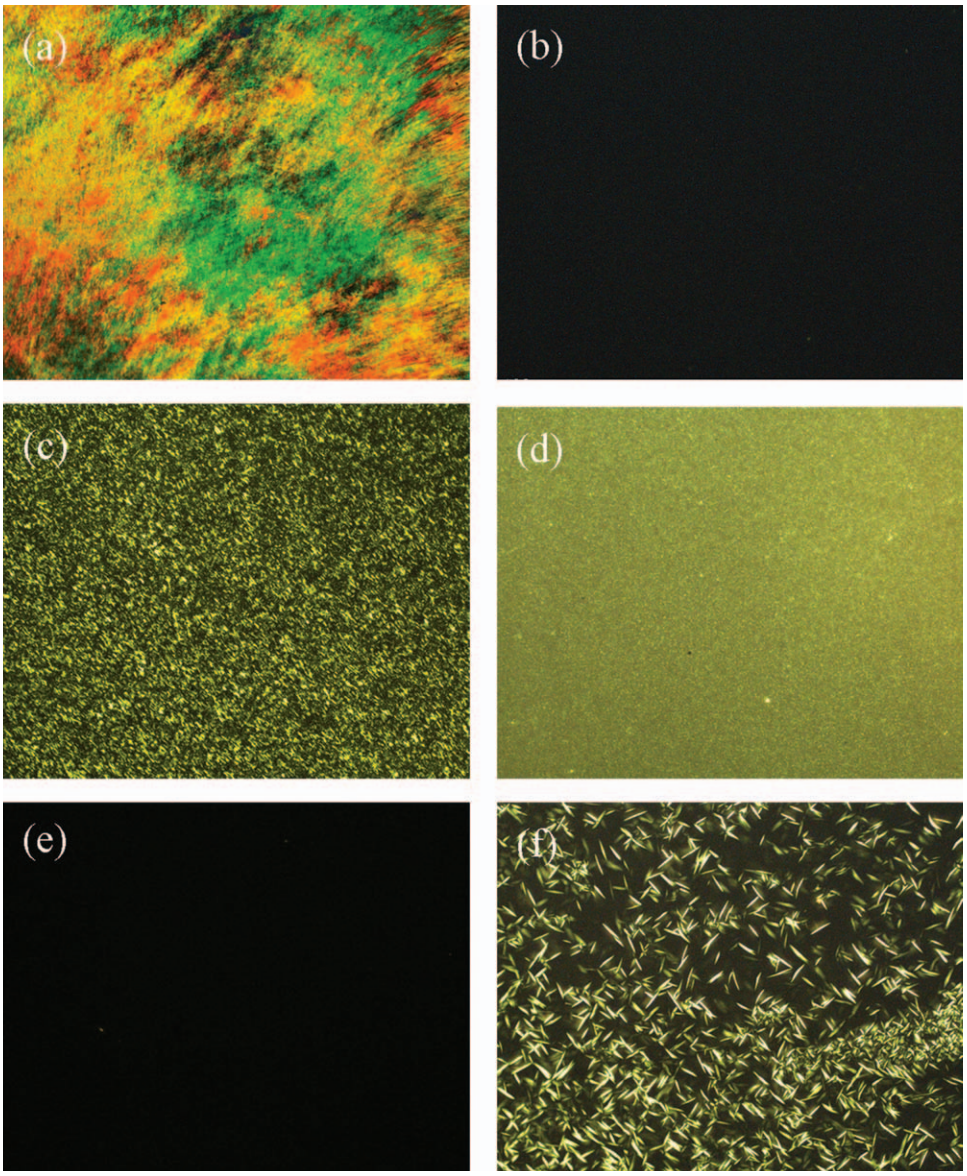

FIGURE 4 Representative POM images of the texture of the P-OC1 maintained at 200 °C (a), representative POM images of the texture of P-OC4 maintained at 130 °C (b), 169 °C (c) and representative POM images of the texture of the P-OC10 maintained at 127 °C (d), 145 °C (e), 260 °C (f) (Magnification: ×200).

However, the relationship between alkyl length and T_g of the P-OC*m* is confusing. Usually, the T_g decreases gradually with an increasing length of the alkyl tails as a result of decreased packing density imposed by the enhanced internal plasticization, however, it can be seen from Figure 3(b) that the changes of T_g is not regular. First, the T_g of P-OC*m* ($m = 1$, 2, 4, and 6) were decreased with the increase in the length of alkyl; then were increased with the increase in m for P-OC*m* ($m = 6$, 8, and 10) and were decreased with further increase in alkyl length for P-OC*m* ($m = 10$, 12, 14, 16, and 18) in the end. So, the changes of T_g is very interesting, we would further prove the results through the solid ^{13}C NMR.[66]

POM experiments further confirm the DSC results. From the POM experiences, it also clears that they can be divided into three types. First, for the samples P-OC*m* ($m = 1$ and 2) exhibited the stable texture. The liquid crystalline birefringence of P-OC1 unchanged even when heated to 300 °C [Fig. 4(a)]. While cooled to room temperature from 300 °C, the birefringence of the sample remained unchanged. Second, for the samples P-OC*m* (m=4, 6, and 8) showed the isotropic phase and LC phase. Figure 4(b,c) shows the observation for sample P-OC4. On heating, the sample becomes soft above the T_g but there is no birefringence [Fig. 4(b)]. The LC texture is formed only when the temperature reaches about 169 °C [Fig. 4(c)] at which a corresponding endotherm appears in DSC curve. On heating further, no visible change of birefringence is observed before decomposition (onset temperature > 300 °C). On the subsequent cooling, the original scene is reestablished; that is, the birefringence

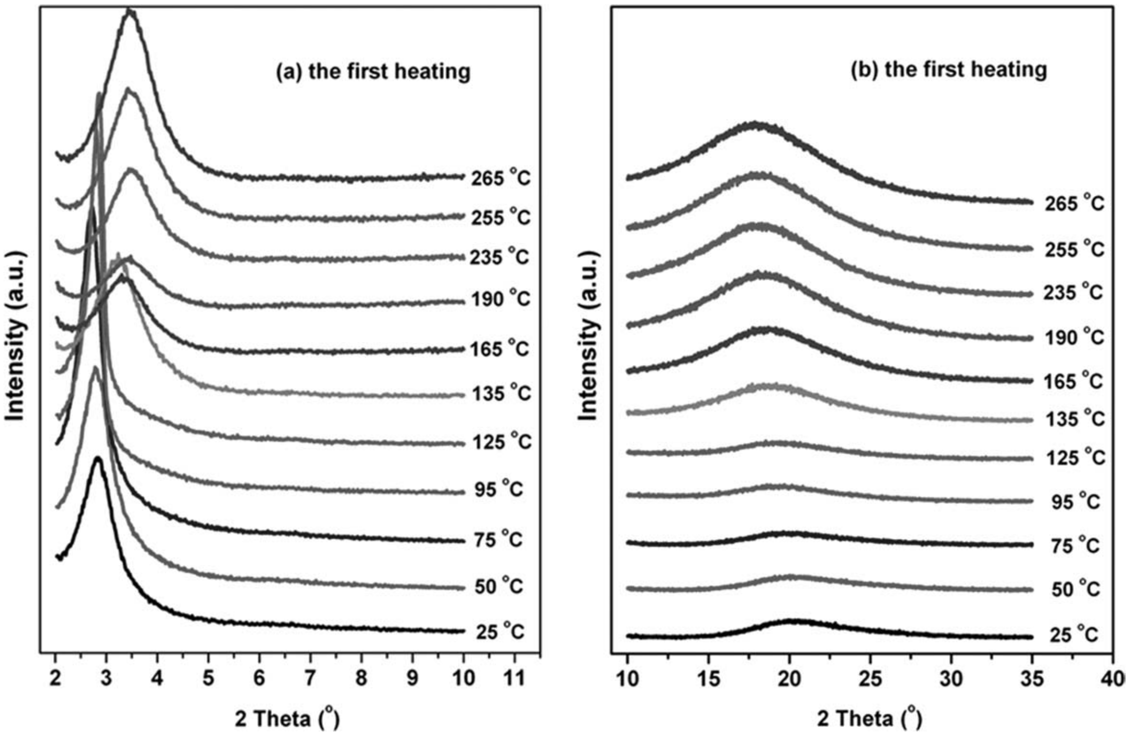

FIGURE 5 One-dimensional WAXD patterns of the P-OC10 during the first heating process of the as-cast film [(a) in the low 2θ and (b) in the high 2θ].

disappears. As for these, two kinds of the samples with short alkoxy tails are well consistent with the previous works.[60,62] Third, for the samples P-OC*m* (m = 10, 12, 14, 16, and 18) presented a thermodynamically stable isotropic phase between two LC phases at lower and higher temperature. Herein, we use the P-OC10 as an example to describe the textures of the third type of polymers observed by POM [see Fig. 4(d–f)]. The phase behaviors and transition temperatures from the POM results are perfectly consistent with the DSC experiments. It is worth noticing that the two liquid crystalline phases of P-OC10 that came up at lower and higher temperature were different and the textures developed more perfectly at higher temperature than the lower temperature. Moreover, as for the P-OC18, we can observe the crystal of long alkoxy tail (see Supporting Information Fig. S1).

To elucidate the phase structures and transitions clearly, WAXD experiments at different temperatures were performed to identify the corresponding structural evolutions. In these experiments, about 30 mg of polymer were cast from THF solution. The results of 1D WAXD data for P-OC*m* (m = 1, 2, 4, 6, and 8) are the same as the previous papers,[62] herein, we would not discuss the experiment results again. Figure 5(a,b) illustrates the 1D WAXD patterns of the as-cast sample (P-OC10) obtained during the first heating process. As shown in Figure 5(a), below 135 °C the diffraction intensity at low 2θ value of 2.81° (d = 3.14 nm) gradually increased with the increase in the temperature; between 135 °C and 190 °C, the diffraction peak became a very diffuse and weak scattering halo, indicating a transition from ordered state to isotropic state. However, with further increase in the temperature, the diffraction peak gradually developed again, indicating the formation of another ordered structure. In Figure 5(b), the amorphous halo in the higher 2θ range presented similar transitions as the diffraction at low 2θ range, that is, first, the halo gradually become broader, then gradually become narrower and the center of halo is found to shift to lower 2θ range with the increasing temperature. The similar features were observed during the cooling process and the experiment results omitted here. This special phenomenon agrees well with the results of POM and DSC. It is noted that the value of the diffraction peaks at lower temperature and higher temperature was different, that is, the diffraction peaks remained about 2.81° (d = 3.14 nm) with lightly thermal expansion at lower temperature and the diffraction peaks appeared about 3.47° (d = 2.55 nm) at higher temperature, indicating two different LC phases. At lower temperature, the ordered structure is mystical to us at this moment, however, at higher temperature, the polymer form the typical column phase similar to the other MJLCPs. Unfortunately, because of the temperature control unit (Paar Physica TCU 100) in conjunction with the diffractometer only cool to room temperature, herein, we cannot observe the crystallization for the sample.

With the increase in length of alkoxy flexible terminals, the crystallization phenomenon of longer alkoxy tails could be detected by the WAXD, so WAXD experiments for P-OC*m* (m = 16 and 18) provided the different information about

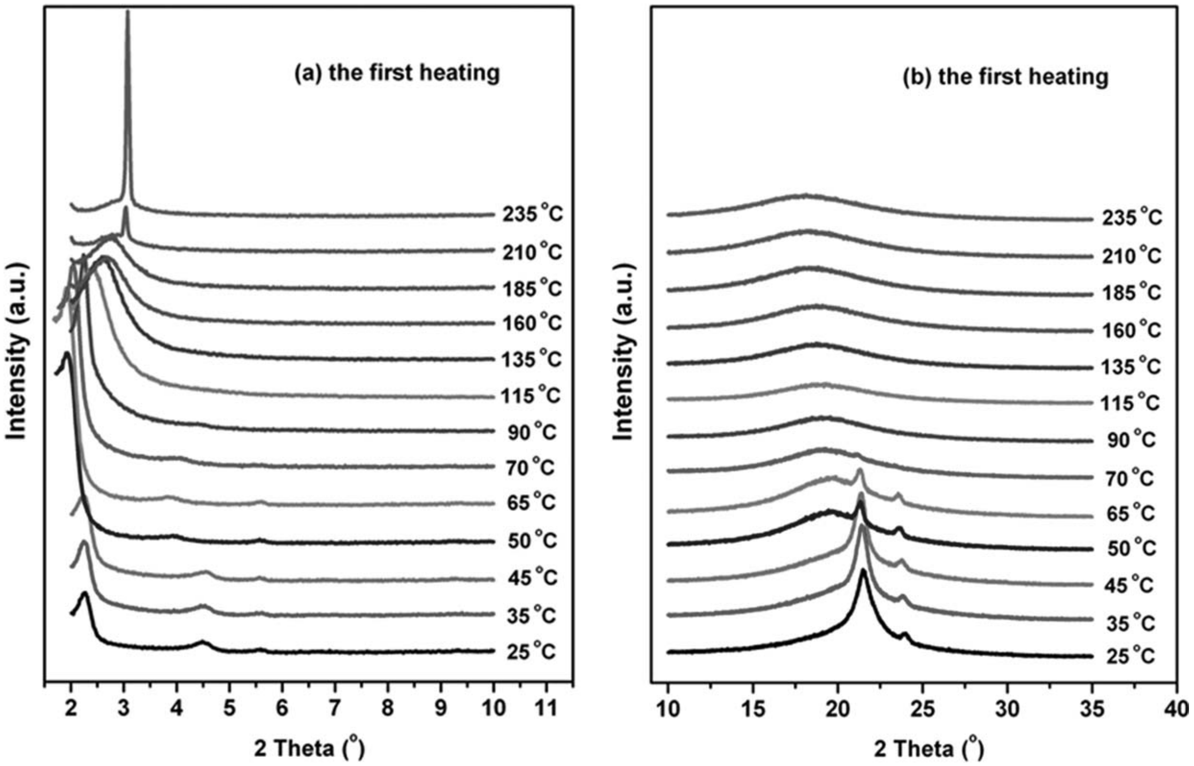

FIGURE 6 One-dimensional WAXD patterns of the P-OC18 obtained during the first heating process of the as-cast film [(a) in the low 2θ and (b) in the high 2θ].

the changes of structural relative to the P-OC10. Herein, we use the P-OC18 as an example [see Fig. 6(a,b)] to elucidate the structural evolution. At lower temperature range, the WAXD patterns only rendered several peaks [as shown in Fig. 6(b)] in the high 2θ region of 10–35°, indicating the typical crystal formed by the long alkoxy tails.[64,67,68] In the low 2θ region of 3–6° [as shown in Fig. 6(a)], three obvious diffraction peaks were observed. The ratio of scattering vectors of the first diffraction peaks and the second was 1:2, indicating a lamellar structure which was similar to the structure formed by hairy-rod.[52,69] When the sample was heated to 70 °C, several peaks in Figure 6(b) gradually disappeared and the residual diffraction halo gradually shift to lower 2θ region, but the ratio of the scattering in Figure 6(a) was still 1:2, implying that the crystal between the lamellar structure gradually melted, but the lamellar structure still remained and the scale of d-spacing gradually increased. We can calculate the value of (100) diffraction is 3.95 nm, which is almost equal to the theoretic value 3.94 nm. As for the theoretic value, it is calculated by two points. One is that the length of rigid core is about 1.92 nm. Conversely, with increasing per two methylene, the length of side chain will increase 0.25 nm when the alkane takes trans conformation. According to the scale of d-spacing and the theoretic value, the polymer basically formed one-layer structure. Further increasing the temperature, only one diffraction halo left and became a very diffuse and weak scattering halo in Figure 6(a,b), indicating a transition from LC state to isotropic state. However, a new diffraction around 3.03° ($d = 2.92$ nm) presented when the temperature was heated to 210 °C, illuminating a column liquid crystalline phase was formed. The similar phenomenon was observed on the cooling process. Based on the WAXD data, we can calculate the value of (100) diffraction for samples P-OC10, P-OC12, P-OC14, and P-OC16 are 3.14, 3.23, 3.43, and 3.67 nm, which are almost equal to the theoretic value 2.94, 3.19, 3.44, and 3.69 nm. Therefore, we may speculate the mystical phase should be smectic A phase. So, four phases for the samples P-OC*m* ($m = 10$, 12, 14, 16, and 18) subject to crystal, smectic A phase, isotropic phase and column phase.

To further confirm the phase transition and information about the nature of various phases, rheological measurements were performed. Because the sample was not enough, we renewably synthesized the sample P-OC18^f (molecular characteristics of P-OC18^f can be seen in Table 1). The molecular weight of the polymer affected the transition temperatures which has been researched by our group, but did not influence the change of the phase dynamics from the phase to the other phase. Thereafter, the sample P-OC18^f was loaded into the instrument at 160 °C and cooled to 90 °C. Temperature dependences of the shear storage modulus G', loss modulus G'' and complex viscosity Eta* were recorded at a rate of 10 °C/min in Figure 7(b). The transition temperatures evaluated by DSC at a rate of 10 °C/min in Figure 7(a). It can be seen that two peaks shape of modulus and complex viscosity are seen around T_1 and T_2, which agrees well with the transition temperature of this polymer on DSC

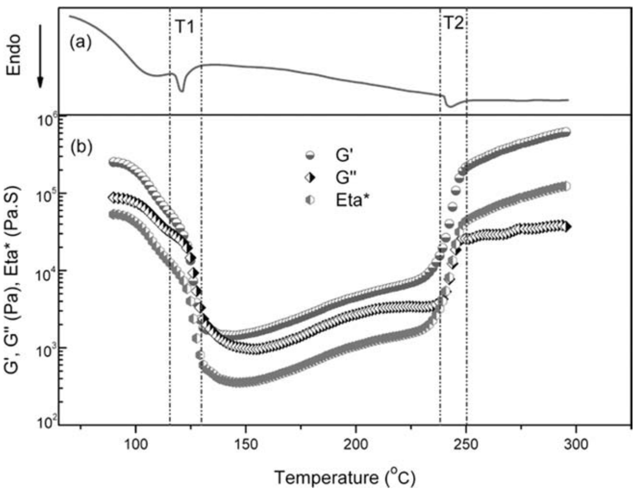

FIGURE 7 Heat flow at a heating rate 10 °C/min in DSC (a) and temperature dependence of *G*′, *G*″, and Eta* for during heating from 90 °C to 290 °C in rheology (b). Conditions: 1% strain, 10 rad/s frequency and 10 °C/min heating rate.

scan. First, before the temperature T_1, G', G'', and Eta* slightly decrease with the increase in temperature. Around T_1, a dramatic decrease in the modulus and viscosity is observed. It clearly indicates a phase transition; moreover, due to the low viscosity of isotropic phase, it also excludes any known optically isotropic cubic phases which are highly viscous. More ordered smectic phases are known to show higher viscosity values than an isotropic phase.[70,71] So, the transition shape is a evidence of a smectic to isotropic phase transition. Second, the modulus and viscosity slightly increase between T_1 and T_2. Third, a dramatic increase in the modulus and viscosity is observed around T_2, indicating isotropic phase to the other phase, followed by a slight increase at higher temperature. In addition, the storage modulus is significantly greater than the loss modulus when the temperature beyond T_2.

The properties of the low temperature LC phase, isotropic phase, and the high temperature LC phase are characterized by the frequency dependence of G' and G'' as well as the Eta* which are shown in Figure 8. The frequency sweeps (0.1–100 rad/s) for various states of the samples were performed at 95, 105, 115, 170, and 260 °C. It can be seen from Figure 8(b–d), there are difference to G', G'', and Eta* versus frequency when the polymers enter the different phase state. The data recorded at 105 °C show the linear viscoelastic response, highly shear thinning behavior for the complex viscosity, with the storage modulus greater than the loss modulus. The change of the viscoelastic properties of the polymer is similar from 95 to 115 °C, which are shown

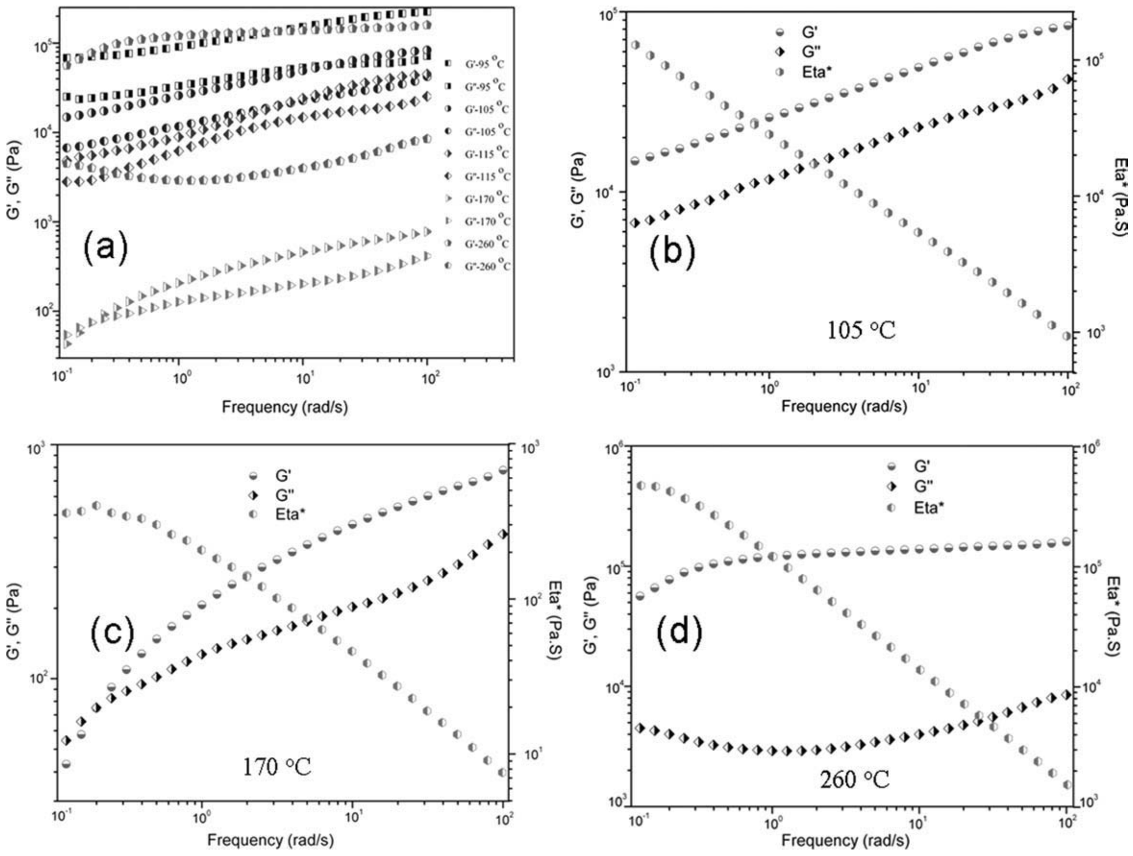

FIGURE 8 Dependence of the shear moduli on frequency; the temperature (°C) is marked on each frequency sweep (a). Frequency dependencies of the storage modulus, loss modulus, and complex viscosity at 105 (b), 170 (c), and 260 °C (d).

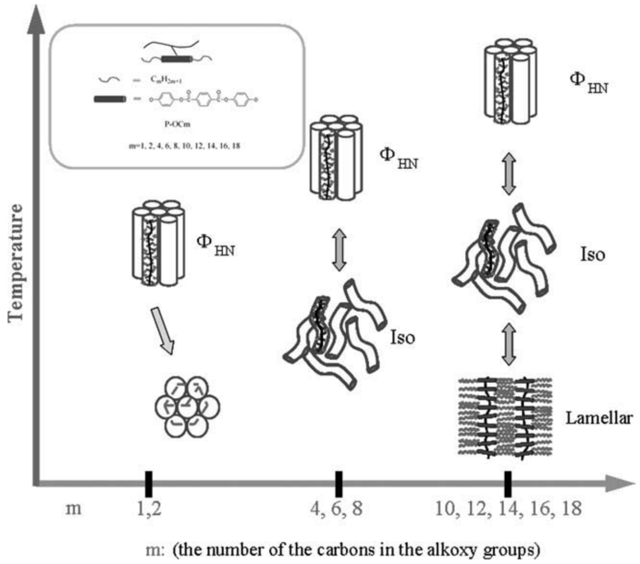

FIGURE 9 Schematic drawing of the thermotropic phase behavior of the polymers.

in Figure 8(a), which is very similar to those usually observed for flexible homopolymers in smectic layer state.[72] The data recorded at 170 °C indicate the terminal regime at low frequency which is observed in the isotropic state for flexible polymers. The data recorded at 260 °C show that the storage modulus and the loss modulus are essentially independent of frequency, with the storage modulus greater than the loss modulus. As for this, it may be reasonable that the single molecule acts as a rigid unit form columnar nematic phase.[60]

Phase Structure Evolution: Influence of Difference of Alkyl-Tail Lengths

Based on DSC, POM, XRD, and ARES rheometer experiments results, P-OC*m* ($m = 1$, 2, 4, 6, 8, 10, 12, 14, 16, and 18) exhibits three types of different behaviors with the increasing length of alkoxy flexible terminals, as shown in Figure 9. The first type is that polymers show the transitional MJLCP phase behavior when polymers have the short alkoxy terminals containing one and two carbon atoms, which is attributed to a cooperative assembly of the backbone and its laterally attached mesogenic groups. The second type is that polymers present a re-entrant isotropic phase and a LC phase when the length of alkoxy tails become four to eight carbon atoms. The LC phase of these polymers is formed through a global change of the whole molecule from the coiled to extended chain conformation accompanied by an increase of the entropy which originates from the free mobilities of bulky side chains in LC phase. The last type is that the P-OC*m* ($m = 10$, 12, 14, 16, and 18) exhibits a re-entrant isotropic phase and two different kinds of LC. As for the appearance and disappearance of this re-entrant isotropic phase, it is considered to be the competing between the microphase separation and the driving force of the entropy over a specific temperature range. Although the reentrant isotropic has been already reported in large disk-like molecules,[73,74] oligomers,[75] and poly(*r*-benzyl L-glutamate)[76] which exhibits a re-entrant isotropic phase in certain mixed solvents such as dichloroacetic acid + dichloroethane, it is difficult to find the re-entrant isotropic phase in the thermotropic LC polymer system. Therefore, it may be useful to understand the re-entrant phase in the thermotropic LC polymer system through studying the phase behavior of the MJLCPs.

CONCLUSIONS

We have successfully synthesized a series of vinyl monomers M-OC*m* ($m = 1$, 2, 4, 6, 8, 10, 12, 14, 16, and 18) containing different length of alkoxy terminal chains. On using conventional radical polymerization, we further obtained the corresponding MJLCPs. The chemical structures of the monomers and polymers were confirmed by various characterization techniques. The phase structures and transitions of these polymers were investigated by the combined technology of DSC, POM, WAXD, and ARES rheometer. The experimental results reveal that MJLCPs can form a re-entrant isotropic phase which is separating smectic phase and columnar phases in one polymer because of the microphase separation and the driving force of the entropy. In low temperature, with increasing length of alkoxy tails on the mesogen, the flexible terminal substituents are increasingly immiscible with the rigid core. Thus polymers form the smectic phase based on self-assembly layers. In high temperature, due to the driving force of the entropy, hairy-rod polymers form the columnar phase in which alkoxy tails and rigid core become a unit. Rheological measurement shows that the MJLCPs have the lower dynamic moduli and complex viscosity in re-entrant isotropic phase. As for the conformational transition of the alkyl side chains, relationship between the alkyl side chains and the main chain, and the phase behaviors and structures of this type of MJLCPs with different density and position of the long alkoxy tails attached to their side-chain rigid-rods, detailed study will be done in our further research.

ACKNOWLEDGMENT

This research was financially supported by the Innovation Platform Open Foundation of University of Hunan Province (10k067), the National Nature Science Foundation of China (51073131, 21174117, 21104062). The authors thank Chen Er-Qiang of Peking University for his help with WAXD experiments measurements.

REFERENCES AND NOTES

1 Beiner, M.; Huth, H. *Nat. Mater.* **2003,** *2*, 595–599.

2 Percec, V.; Rudick, J. G.; Peterca, M.; Heiney, P. A. *J. Am. Chem. Soc.* **2008,** *130*, 7503–7508.

3 Percec, V.; Bera, T. K.; Glodde, M.; Fu, Q. Y.; Balagurusamy, V. S. K.; Heiney, P. A. *Chem. Eur. J.* **2003,** *9*, 921–935.

4 Ungar, G.; Percec, V.; Holerca, M. N.; Johansson, G.; Heck, J. A. *Chem. Eur. J.* **2000,** *6*, 1258–1266.

5 Percec, V.; Dulcey, A. E; Balagurusamy, V. S. K.; Miura, Y.; Smidrkal, J.; Peterca, M.; Nummelin, S.; Edlund, U.; Hudson, S. D.; Heiney, P. A.; Hu, D. A.; Magonov, S. N.; Vinogradov, S. A. *Nature* **2004,** *430*, 764–768.

6 Percec, V.; Ahn, C. H.; Ungar, G.; Yeardley, D. J. P.; Moller, M.; Sheiko, S. *Nature* **1998,** *391*, 161–164.

7 Percec, V.; Heck, J.; Lee, M.; Ungarb, G.; Alvarez-Castillob, A. *J. Mater. Chem.* **1992,** *2*, 1033–1039.

8 Percec, V.; Tomazos, D.; Heck, J.; Blackwell, H.; Ungar, G. *J. Chem. Soc. Perkin. Trans.* **1994,** *2*, 31–44.

9 Chen, X. F.; Shen, Z. H.; Wan, X. H.; Fan, X. H.; Chen, E. Q.; Ma, Y. G.; Zhou, Q. F. *Chem. Soc. Rev.* **2010,** *39*, 3072–3101.

10 Percec, V.; Aqad, E.; Peterca, M.; Rudick, J. G.; Lemon, L.; Ronda, J. C.; De, B. B.; Heiney, P. A.; Meijer, E. W. *J. Am. Chem. Soc.* **2006,** *128*, 16365–16372.

11 Prokhorova, S. A.; Sheiko, S. S.; Ahn, C. H.; Percec, V.; Moller, M. *Macromolecules* **1999,** *32*, 2653–2660.

12 Percec, V.; Schlueter, D.; Ungar, G.; Cheng, S. Z. D.; Zhang, A. *Macromolecules* **1998,** *31*, 1745–1762.

13 Percec, V.; Schlueter, D.; Ronda, J. C.; Johansson, G.; Ungar, G.; Zhou, J. P. *Macromolecules* **1996,** *29*, 1464–1472.

14 Percec, V.; Cho, W. D.; Mosier, P. E.; Ungar, G.; Yeardley, D. J. P. *J. Am. Chem. Soc.* **1998,** *120*, 11061–11070.

15 Rosen, B. M.; Wilson, C. J.; Wilson, D. A.; Peterca, M.; Imam, M.A.; Percec. V. *Chem. Rev.* **2009,** *109*, 6275–6540.

16 Percec, V.; Imam, M. A.; Peterca, M.; Leowanawat, P. *J. Am. Chem. Soc.* **2012,** *134*, 4408–4420.

17 Percec, V.; Aqad, E.; Peterca, M.; Rudick, J. G.; Lemon, L.; Ronda, J. C.; De, B. B.; Heiney, P. A.; Meijer, E. W. *J. Am. Chem. Soc.* **2006,** *128*, 16365–16372.

18 Peterca, M.; Imam, M. A.; Leowanawat, P.; Rosen, B. M.; Wilson, D. A.; Wilson, C. J.; Zeng, X. B.; Ungar, B.; Heiney, P. A.; Percec, V. *J. Am. Chem. Soc.* **2010,** *132*, 11288–11305.

19 Balagurusamy, V. S. K.; Ungar, G.; Percec, V.; Johansson, G. *J. Am. Chem. Soc.* **1997,** *119*, 1539–1555.

20 Percec, V.; Peterca, M.; Dulcey, A. E.; Imam, M. R.; Hudson, S. D.; Nummelin, S.; Adelman, P.; Heiney, P. A. *J. Am. Chem. Soc.* **2008,** *130*, 13079–13094.

21 Rudick, J. G.; Percec, V. *Acc. Chem. Res.* **2008,** *41*, 1641–1652.

22 Rapp, A.; Schnell, I.; Sebastiani, D.; Brown, S. P.; Percec, V.; Spiess, H. W. *J. Am. Chem. Soc.* **2003,** *125*, 13284–13297.

23 Zhou, Q. F.; Li, H. M.; Feng, X. D. *Macromolecules* **1987,** *20*, 233–234.

24 Zhou, Q. F.; Zhu, X. L.; Wen, Z. Q. *Macromolecules* **1989,** *22*, 491–493.

25 Zhu, Z. G.; Zhi, J. G.; Liu, A. H.; Cui, J. X.; Tang, H.; Qiao, W. Q.; Wan, X. H.; Zhou, Q. F. *J. Polym. Sci. Part A: Polym. Chem.* **2007,** *45*, 830–847.

26 Ye, C.; Zhang, H. L.; Huang, Y.; Chen, E. Q.; Lu, Y. L.; Shen, D. Y.; Wan, X. H.; Shen, Z. H.; Cheng, S. Z. D.; Zhou, Q. F. *Macromolecules* **2004,** *37*, 7188–7196.

27 Chai, C. P.; Zhu, X. Q.; Wang, P.; Ren, M. Q.; Chen, X. F.; Xu, Y.-D.; Fan, X. H.; Ye, C.; Chen, E. Q.; Zhou, Q. F. *Macromolecules* **2007,** *40*, 9361–9370.

28 Xu, Y. D.; Yang, Q.; Shen, Z. H.; Chen, X. F.; Fan, X. H.; Zhou, Q. F. *Macromolecules* **2009,** *42*, 2542–2550.

29 Wang, X. Z.; Zhang, H. L.; Chen, E. Q.; Wang, X. Y.; Zhou, Q. F. *J. Polym. Sci. Part A: Polym. Chem.* **2005,** *43*, 3232–3244.

30 Guan, Y.; Chen, X. F.; Shen, Z. H.; Wan, X. H.; Zhou, Q. F. *Polymer* **2009,** *50*, 936–944.

31 Chen, X. F.; Tenneti, K. K.; Li, C. Y.; Bai, Y. W.; Zhou, R.; Wan, X. H.; Fan, X. H.; Zhou, Q. F. *Macromolecules* **2006,** *39*, 517–527.

32 Gopalan, P.; Andruzzi, L.; Li, X.; Ober, C. K. *Macromol. Chem. Phys.* **2002,** *203*, 1573–1583.

33 Cheng, Y. H.; Chen, W. P.; Shen, Z. H.; Fan, X. H.; Zhu, M. F.; Zhou, Q. F. *Macromolecules* **2011,** *44*, 1429–1437.

34 Stern, R.; Ballauff, M.; Lieser, G.; Wegner, G. *Polymer* **1991,** *32*, 2096–2105.

35 Duran, R.; Ballauff, M.; Wenzel, M.; Wegner, G. *Macromolecules* **1988,** *21*, 2897–2899.

36 Galda, P.; Kistner, D.; Martin, A.; Ballauff, M. *Macromolecules* **1993,** *26*, 1595–1602.

37 Voigt-Martin, I. G.; Simon, P.; Bauer, S.; Ringsdorf, H. *Macromolecules* **1995,** *28*, 236–242.

38 Ballauff, M.; Schmidt, G. F. *Makromol. Chem. Rapid Commun.* **1987,** *8*, 93–97.

39 Wendorff, J. H.; Hermann, S. O. *Makromol. Chem. Rapid Commun.* **1986,** *7*, 791–796.

40 Zheng, W.Y.; Levon, K.; Taka, T.; Laakso, J.; Österholm, J. E. *J. Polym. Sci. Part B: Polym. Phys.* **1994,** *33*, 1289–1306.

41 Zheng, W. Y.; Levon, K.; Laakso, J.; Österholm, J. E. *Macromolecules* **1994,** *27*, 7754–7768.

42 Qiao, X. Y.; Wang, X. H.; Mo, Z. S. *Synth. Met.* **2001,** *118*, 89–95.

43 Pankaj, S.; Hempel, E.; Beiner, M. *Macromolecules* **2009,** *42*, 716–724.

44 Kricheldorf, H. R; Domschke, A. *Macromolecules* **1996,** *29*, 1337–1344.

45 Kricheldorf, H. R; Domschke, A. *Macromolecules* **1994,** *27*, 1509–1516.

46 Espenschied, B.; Schulz, R. C. *Polym. Bull.* **1981,** *15*, 489–495.

47 Espenschied, B.; Schulz, R. C. *Makromol. Chem. Rapid. Commun.* **1983,** *4*, 633–638.

48 Watanabe, J. J.; Sekine, N.; Nematsu, T.; Sone, M.; Kricheldorf, H. R. *Macromolecules* **1996,** *29*, 4816–4818.

49 Sone, M.; Wada, T.; Harkness, B. R.; Watanabe, J. J.; Takahashi, H.; Huang, H. W.; Yamashita, T.; Horie, K. *Macromolecules* **1998,** *31*, 8865–8870.

50 Fu, K.; Nematsu, T.; Sone, M.; Itoh, T.; Hayakawa, T.; Ueda, M.; Tokita, M.; Watanabe, J. *Macromolecules* **2000,** *33*, 8367–8370.

51 Watanabe, J. J.; Ono, H.; Uematsu, L.; Abe, A. *Macromolecule* **1985,** *18*, 2141–2148.

52 Stepanyan, R.; Subbotin, A.; Knaapila, M.; Ikkala, O.; Brinke, G. T. *Macromolecules* **2003,** *36*, 3758–3763.

53 Damman, S. B.; Vroege, G. J. *Polymer* **1993,** *34*, 2773–2777.

54 Watanabe, J.; Harkness, B. R.; Sone, M.; Ichimura, H. *Macromolecules* **1994,** *27*, 507–512.

55 Sone, M.; Harkness, B. R.; Kurosu, H.; Ando, I.; Watanabe, J. *Macromolecules* **1994,** *27*, 2769–2777.

56 Jansen, J. C.; Addink, R.; Nijenhuis, K.; Mijs, W. J. *Macromol. Chem. Phys.* **1999,** *200*, 1473–1484.

57 Chen, S.; Gao, L. C.; Zhao, X. D.; Chen, X. F.; Fan, X. H.; Xie, P. Y.; Zhou, Q. F. *Macromolecules* **2007,** *40*, 5718–5725.

58 Chen, S.; Zhang, L. Y.; Gao, L. C.; Chen, X. F.; Fan, X. H.; Shen, Z. H.; Zhou, Q. F. *J. Polym. Sci. Part A: Polym. Chem.* **2009,** *47*, 505–514.

59 Zhang, L. Y.; Shen, Z. H.; Fan, X. H.; Zhou, Q. F. *J. Polym. Sci. Part A: Polym. Chem.* **2011,** *49*, 3207–3217.

60 Zhao, Y. F.; Fan, X. H.; Wan, X. H.; Chen, X. F.; Yi, Y.; Wang, L. S.; Dong, X.; Zhou, Q. F. *Macromolecules* **2006,** *39*, 948–956.

61 Zhang, H.; Yu, Z.; Wan, X.; Zhou, Q. F.; Woo, E. M. *Polymer* **2002,** *43*, 2357–2361.

62 Zhang, D.; Liu, Y. X.; Wan, X. H.; Zhou, Q. F. *Macromolecules* **1999,** *32*, 5183–5185.

63 Klarmann, E.; Catyas, L. W.; Shternov, V. A. *J. Am. Chem. Soc.* **1932,** *54*, 298–305.

64 Shi, H. F.; Zhao, Y.; Zhang, X. Q.; Zhou, Y. Y.; Xu, Z.; Zhou, S. R.; Wang, D. J.; Han, C.; Xu, D. F. *Polymer* **2004,** *45*, 6299–6307.

65 Kaufman, H. S.; Sacher, A.; Alfrey, T.; Fankuchen, I. *J. Am. Chem. Soc.* **1948,** *70*, 3147–3147.

66 Okabe, A.; Yamanobe, T.; Watanabe, J.; Ando, I. J. *Mol. Struct.* **1989,** *213*, 213–220.

67 Shi, H. F.; Zhao, Y.; Jiang, S. C.; Xin, J. H.; Rottstegge, J.; Xu, D. F.; Wang, D. J. *Polymer* **2007,** *48*, 2762.

68 Lopez-Carrasquero, F.; Martinez de Ilarduya, A.; Cardenas, M.; Carrillo, M.; Arnal, M. L.; Laredo, E.; Torres, C.; Mendez, B.; Muller, A. J. *Polymer* **2003,** *44*, 4969–4979.

69 Knaapila, M.; Stepanyan, R.; Horsburgh, L. E.; Monkman, A. P.; Serimaa, R.; Ikkala, O.; Subbotin, A.; Torkkeli, M.; Ten Brinke, G. *J. Phys. Chem. B.* **2003,** *107*, 14199–14203.

70 Hudson, S. D; Lovinger, A. J.; Larson, R. G.; Davis, D. D.; Garay, R. O.; Fujishiro K. *Macromolecules* **1993,** *26*, 5643–5650.

71 Alt, D. J.; Hudson, S. D.; Garay, R. O.; Fujishiro K. *Macromolecules* **1995,** *28*, 1575–1579.

72 Craig, A. A.; Winchester, L.; Madden, P. C.; Larcey, P.; Hamley, L. W.; Imrie, C. T. *Polymer* **1998,** *39*, 1197–1205.

73 Pietrasik, U.; Szydlowska, J.; Krowczynski, A.; Pociecha, D.; Gorecka, E.; Guillon, D. *J. Am. Chem. Soc.* **2002,** *124*, 8884–8890.

74 Pietrasik, U.; Szydlowska, J.; Krowczynski, A. *Chem. Mater.* **2004,** *16*, 1485–1492.

75 Percec, V.; Lee, M.; Heck, J.; Blackwell, H. E.; Ungar, G.; AlvarezCastillo, A. *J Mater. Chem.* **1992,** *2*, 931–938.

76 Lin, J. P.; Abe, A. *Macromolecules* **1996,** *29*, 2584–2589.